Final Draft
of the original manuscript:

Krüger-Genge, A.; Dietze, S.; Yan, W.; Liu, Y.; Fang, L.; Kratz, K.; Lendlein, A.; Jung, F.:

Endothelial cell migration, adhesion and proliferation on different polymeric substrates.

In: Clinical Hemorheology and Microcirculation. Vol. 70 (2019) 4, 511 - 529.
First published online by IOS: February 22, 2019

10.3233/CH-189317
https://dx.doi.org/10.3233/CH-189317

Endothelial cell migration, adhesion and proliferation on different polymeric substrates

Anne Krüger-Genge[1¶†], Stefanie Dietze[1¶£], Wan Yan[1,2], Yue Liu[1,2], Liang Fang[1±], Karl Kratz[1], Andreas Lendlein[1,2], Friedrich Jung[1*]

1 Institute of Biomaterial Science and Berlin-Brandenburg Center for Regenerative Therapies, Helmholtz-Zentrum Geesthacht, Teltow, Germany
2 Institute of Chemistry, University of Potsdam, Potsdam, Germany

*Corresponding author: Prof. Dr. F. Jung, Institute of Biomaterial Science and Berlin-Brandenburg Center for Regenerative Therapies, Helmholtz-Zentrum Geesthacht, Teltow, Germany. E-Mail: friedrich.jung@hzg.de

¶ These authors contributed equally

† present address: Department of Anestesia, Pain Management and Perioperative Medicine, Faculty of Medicine, Dalhousie University, Halifax, Canada

£ Present address: Berlin Heart GmbH, Berlin, Germany

± Present address: College of Materials Science and Engineering, Nanjing Tech University, Nanjing 210009, PR China

Abstract

Background: The formation of a functionally-confluent endothelial cell (EC) monolayer affords proliferation of EC, which only happens in case of appropriate migratory activity.
Aim of the study: The migratory pathway of human umbilical endothelial cells (HUVEC) was investigated on different polymeric substrates.
Material and Methods: Surface characterization of the polymers was performed by contact angle measurements and atomic force microscopy under wet conditions. 30,000 HUVEC per well were seeded on polytetrafluoroethylene PTFE (θ_{adv} = 119° ± 2°), on low-attachment plate LAP (θ_{adv} = 28° ± 2°) and on polystyrene based tissue culture plates (TCP, θ_{adv} = 22° ± 1°). HUVEC tracks (trajectories) were recorded by time lapse microscopy and the euclidean distance (straight line between starting and end point), the total distance and the velocity of HUVEC not leaving the vision field were determined.
Results: On PTFE, 42 HUVEC were in the vision field directly after seeding. The mean length of single migration steps (SML) was 6.1 ± 5.2 µm, the mean velocity (MV) 0.40 ± 0.3 µm·min^{-1} and the complete length of the trajectory (LT) was 710 ± 440 µm. On TCP 82 HUVEC were in the vision field subsequently after seeding. The LT was 840 ± 550 µm, the SML 6.1 ± 5.2 µm and the MV 0.44 ± 0.3 µm·min^{-1}. The trajectories on LAP differed significantly in respect to SML (2.4 ± 3.9 µm, $p < 0.05$), the MV (0.16 ± 0.3 µm·min^{-1}, $p < 0.05$) and the LT (410 ± 300 µm, $p < 0.05$), compared to PTFE and TCP. Solely on TCP, a nearly confluent EC monolayer developed after three days. While on TCP diffuse signals of vinculin were found over the whole basal cell surface organizing the binding of the cells by focal adhesions, on

PTFE vinculin was merely arranged at the cell rims, and on the hydrophilic material (LAP) no focal adhesions were found.
Conclusion: The study revealed that the wettability of polymers affected not only the initial adherence but also the migration of EC, which is of importance for the proliferation and ultimately the endothelialization of polymer-based biomaterials.

Key words: Endothelial cells, migration, polymer-based biomaterials, cytokine release

1. Introduction

Coronary or peripheral artery disease and related revascularization procedures are still increasing due to the aging of the population and the growing incidence of somatic cardiovascular risk factors like diabetes mellitus [1,2]. Up to now, autologous saphenous veins are the vessels of choice for arterial by-passes [3]. Synthetic vascular grafts like poly(ethylene terephthalate) and expanded polytetrafluoroethylene (ePTFE) are used if vein access cannot be obtained. These synthetic grafts are successfully used to replace large diameter vessels, but they fail in small diameters (<6 mm) [4,5]. It is widely accepted that this occurs due to thrombotic occlusion and intimal hyperplasia [6].

Therefore, different strategies were applied to improve the patency of such grafts. Among those, coatings with molecules to render body foreign surfaces haemocompatible [7-9] or to support the formation of a functionally-confluent layer of endothelial cells (EC) [10-12] were reported. EC seeding on synthetic vascular grafts was introduced in the 1980s, and it was proven to reduce the thrombogenicity of implanted prosthetic grafts [13] and to enhance their patency significantly [14-16].

After seeding of EC on a substrate, endothelialization starts with cell migration, which is described as a three step cycle: first, a membrane protrusion at the leading edge, then adhesion to the substrate and thirdly, the contraction of the cell body [17], which propels the nucleus forward [18] leading to a flow of cytoplasm into the front membrane protrusion [19]. The last step results in a net cell displacement owing to traction on focal adhesions [20]. Step by step EC execute persistent random locomotion until nidation with subsequent spreading and possibly proliferation [21]. If a cell becomes surrounded by other cells, it will stop growing, so that finally in a static culture a “cobblestone” monolayer of polygonal cells at a confluence is created. As a result of these contact-inhibition phenomena, only a fraction of the adherent cells will continue to grow and divide after the initial stages of this process thereby increasing the EC density. This fraction decreases with increasing cell density and depends strongly on cell

motility and substrate characteristics [22]. Therefore, the establishment of an EC monolayer on graft surfaces needs migration, adhesion and spreading of the cells; without migration the EC will not develop a confluent EC monolayer [23].

While there are a lot of studies reporting adherence and EC monolayer formation [24-31], fewer reports are known about their migration, particularly their dependence on the type of the polymeric substrate. Specifically the surface wettability of polymers has been shown to have profound effects upon cell/protein/substrate interactions, with cell adhesion generally preferring surfaces that are less hydrophobic in character [32-36]. As polymer-based substrates hydrophobic ePTFE, a hydrophilic, hydrogel-functionalized polystyrene with ultra-low binding surface (LAP) and corona discharged treated polystyrene (TCP) were explored.

The aim of this study was to investigate whether the migration depends on the hydrophilicity/hydrophobicity of different application-relevant polymeric substrates and if the release of chemokines and cytokines are involved in the process of locomotion. Therefore, human umbilical vein endothelial cells (HUVEC) were cultured on PTFE as an example for an implant material as well as on cell culture materials [hydrophilic modified polystyrene comprising a covalently bound hydrogel on the surface resulting in low protein and cell attachment (LAP) [37] and surface treated polystyrene (TCP)]. The trajectories of isolated cells not leaving the vision field as well as the physiological function of the cells were followed over three days.

2. Material and Methods

2.1. Study design

The migration of well-separated single adherent HUVEC not leaving the vision field was analyzed by a cell-tracking method under static conditions on three different polymeric substrates. Migration of EC requires a temporally coordinated regulation of intracellular components of the cell adhesion apparatus including intracellular and cell-substrate interactions [38]. Therefore, studies concerning the cytokine release as well as the actin cytoskeleton, focal adhesions, and cell-cell contacts were used to complement our microscopic findings. The study was planned and performed in accordance with the ethical guidelines of Clinical Microcirculation and Hemorheology [39].

2.2. Polymeric substrates

A hydrophobic polymer (polytetrafluoroethylene (PTFE)), a hydrophilic polymer (hydrogel-functionalized polystyrene (LAP) with ultra-low binding surface (Corning Inc., Lowell, USA))

and corona discharged treated polystyrene (TCP) (Techno Plastic Products AG, Trasadingen, Switzerland) were used as substrates.

2.3. Contact angle measurements

Dynamic contact angle (DCA) measurements were conducted in ultra-pure de-ionized water with a conductivity of 0.055 µS/cm (Ultra Clear UV clean water system, SG Wasseraufbereitung und Regenerierstation GmbH, Barsbüttel, Germany) at ambient temperature on a drop shape analyzer (DSA 100, Krüss GmbH, Hamburg, Germany) using the captive bubble method. Advancing and receding contact angle measurements were performed by stepwise withdrawing/adding of air from/to the captured bubble, while the bubble was increased with each measurement cycle from 2 to 5 mm in diameter. Prior to the DCA measurement, all samples were preconditioned for 24 hours in de-ionized water at ambient temperature for equilibration. At least five measurements for advancing and receding angles on three different locations were performed for each sample. The average of the contact angles was calculated as well as the standard deviation.

2.4. Atomic force microscopy

Surface topography investigations and local mechanical analysis of the polymeric substrates were performed by AC-mode scanning and nanoindentation using an atomic force microscope (MFP-3D, Asylum Research, Santa Barbara, USA). A BioHeater (Asylum Research, Santa Barbara, USA) was utilized as the sample holder, enabling the measurements in the water at ambient temperature. Before measurements, the AFM components such as the cantilever spring constant and piezoelectric scanner movement were calibrated based on a clean silicon wafer in air and water, while the samples were immersed and equilibrated in de-ionized water at room temperature for 10 min. AC-mode scanning was conducted with OMCL-AC200TS-R3 silicon cantilevers (Olympus, Tokyo, Japan) having a typical spring constant of 9 $N \cdot m^{-1}$ at a scan size of 60 µm x 60 µm with a scan rate of 0.8 or 1.0 Hz. For each sample, scans on three different locations were scanned and the root-mean-square roughness (R_q) of each image was calculated by the software Igor Pro 6.22A (WaveMetrics, Inc., Portland, OR, USA).

Nanoindentation measurements were performed using two different cantilevers. A cantilever (OMCL-AC160-TS-R3, Olympus, Tokyo, Japan) having a spring constant of 25 $N \cdot m^{-1}$ was applied with an indentation force F of 5 µN for investigating the PTFE and TCP samples, and a soft cantilever (MLCT-A, Bruker, Camarillo, USA) with a spring constant of 0.05 $N \cdot m^{-1}$ and $F = 20$ nN was utilized for assessing the mechanics of the hydrogel coating of the LAP substrate. Based on 10 single indentations performed on different locations of each sample average values for the indentation depth (δ), puff-off force (f_p) and the reduced Young's modulus (E) were

obtained. *E* was calculated from the force-distance curves according to the Hertz model by the software Igor Pro 6.22A (WaveMetrics, Inc., Portland, OR, USA). [40,41]

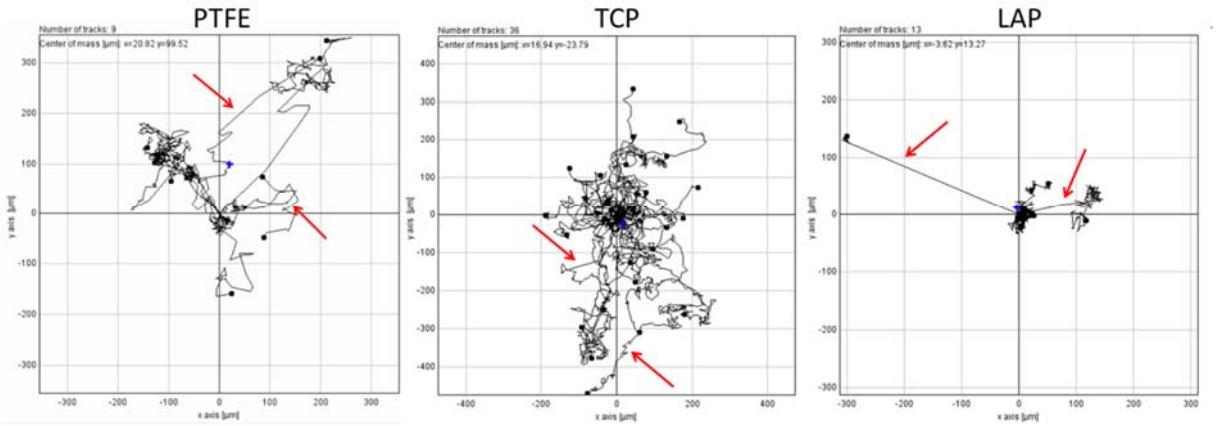

Fig. 1. Representative Cell tracks (trajectories) of HUVEC during migration on PTFE, TCP and LAP for one well each over the observation period of three days. Red arrows refer to migration steps, which were excluded from the analysis

2.5. Endothelial cells

Commercially available human umbilical vein endothelial cells (HUVEC, Lonza, Cologne, Germany) were cultured under static cell culture conditions (37 °C, 5 vol% CO_2) in polystyrene-based cell culture flasks [41]. Cells were used for no longer than 4 passages, cultivating them with endothelial basal medium (EBM-2) supplemented with (Endothelial Growth Medium) EGM-2 Single Quots® kit and 2 vol% FCS (Lonza, Cologne, Germany).

2.6. Experimental set-up

Primary HUVEC (30,000 cells/well) were seeded on the three polymeric materials in a 24-well plate. Subsequently, HUVEC migration was investigated using phase contrast microscopy (Olympus IX 81, Tokyo, Japan) and a microscope incubator (okolab, Ottaviano, Italy) over three days. Since it takes around 10 – 15 minutes until EC have formed their lamella (first step of the migration process according to Lauffenburger [42]), which are needed to start the movement, every 15 minutes an image was taken.

Migration step length, velocity and trajectories length of HUVEC not leaving the vision field of 886 µm x 667 µm were measured according to Stokes et al. [43] using the Manual Tracking- and Chemotaxis Plugin for ImageJ [44]. Single steps greater than the maximal length of HUVEC were excluded from the analysis because such events are most probably detachments with new attachment (see red arrows in Fig. 1). The trajectory ended in case of apoptosis, mitosis, nidation, or when a HUVEC left the vision field during migration, or after detachment and leaving the vision field (only in this case the trajectory was excluded from the analysis).

2.7. Immunocytochemistry

Adherent HUVEC were fixed for 30 minutes in 4 wt% paraformaldehyde (Sigma-Aldrich, Taufkirchen, Germany) after 72 hours of incubation. After permeabilisation using Triton X-100 (0.5 vol%) and blocking of unspecific binding sites with 5% (w/v) bovine serum albumin (BSA, Sigma-Aldrich) in Phosphate buffer saline (PBS, life technologies, Darmstadt, Germany), the samples were incubated with phalloidin-Alexa555 (1:40, Molecular Probes, Darmstadt, Germany) and mouse anti-human vinculin (1:30, Sigma-Aldrich) in 2% (w/v) BSA solved in PBS for 1 hour at room temperature. Secondary antibody donkey anti-mouse coupled with DyLight 488 (1:200, Jackson ImmunoResearch, Hamburg, Germany) was applied after washing. Nuclei were stained using 10 µg/ml 4',6-Diamidin-2-phenylindol (DAPI, Roth, Germany) for 5 minutes. After embedding, the specimen were analyzed using confocal laser scanning microscopy (LSM 510 META, Zeiss, Jena, Germany).

2.8. Proliferation analysis using flow cytometry

For flow cytometry, HUVEC in supernatant as well as adherent HUVEC were used. To measure detachment, adherent HUVEC were washed with PBS, incubated with 0.25 % trypsin/0.53mM EDTA followed by addition of EGM-2. HUVEC in supernatant were centrifuged at 300 x g for 10 minutes and the cell pellet was resolved by adding 70 % of ice-cold ethanol. After incubation for 1 hour at –20 °C, HUVEC were washed twice. Anti-Ki67-FITC and anti-CD31-APC (1:100, both Miltenyi Biotec, Bergisch Gladbach, Germany) antibodies were incubated for 15 minutes at room temperature. After washing and resuspending in autoMACS Running Buffer (Miltenyi Biotec, Germany) measurements were performed at the MACSQuant® analyzer (Miltenyi Biotec, Germany).

2.9. Cytokine secretion

The secretion of cytokines by HUVEC at day 1 and day 3 of cultivation was quantified in the cell culture supernatants using Bioplex Multiplex System (Bio-Plex200®, Bio-Rad, München, Germany) and Bio-Plex Pro Human Cytokine 27-plex assay from Bio-Rad. The analysis was performed according to the manufacturer´s instructions. For every parameter values of the own blank were subtracted from measured values.

2.10. Statistics

For all samples arithmetic mean and standard deviation are given. Categorical variables are presented as percentages.

For the repeated measures two-way ANOVA tests were performed. To isolate the group or groups that differ from the others a multiple comparison procedure was used (Holm-Sidak tests). For three-group comparison one factorial ANOVA was performed.

For comparisons of categorical data between the three groups a 3*2 χ^2 test was performed. Differences were considered significant if *p*-value was less than 0.05.

3. Results

3.1. Surface characteristics of the polymeric substrates

Surface characteristics of the polymeric substrates were analyzed by dynamic contact angle measurements using the captive bubble method and atomic force microscopy (AFM) where the surface roughness and the local mechanical properties were explored under wet conditions (immersed and equilibrated in de-ionized water at room temperature). AFM experiments under wet conditions revealed a surface roughness in the low nanometer range for all investigated substrates with a surface roughness of $R_q = 25 \pm 3.1$ nm for PTFE, while LAP and TCP exhibited a R_q of 8.7 ± 0.7 nm and 10.2 ± 3.1 nm, respectively. The nanomechanical properties of polymeric substrate surfaces were characterized by nanoindentation measurements using AFM and the results are listed in Table 1. TCP samples exhibited the highest values for the reduced Young´s Modulus (E) among the tested samples with 2,480 MPa, followed by PTFE (337 MPa) and the soft hydrogel coating of LAP with $E = 3.5$ MPa. It has to be mentioned that substantial higher E values of 1,530 ± 800 MPa could be determined for some other regions of the LAP substrate. We attribute this high Young´s Modulus to the absence of the hydrogel layer on this particular test region and therefore in this case the mechanics of the underlying polystyrene substrate are investigated. These findings might suggest an inhomogeneous hydrogel coating of the LAP sample. The indentation depth of the different polymeric substrates, which is controlled by the interplay of the materials stiffness and the applied indentation force, varied from 74 ± 16 nm (TCP) to 214 ± 55 nm (LAP) and 345 ± 13 nm for PTFE. Furthermore, the pull-off forces f_p of the different substrates have been explored. f_p represents the adhesive interaction between the cantilever and the tested surface, which is also influenced by the indentation depth. PTFE showed a high f_p of 32.3 ± 10 nN followed by TCP ($f_p = 5.2 \pm 2$ nN) while for LAP a low f_p of 0.6 ± 0.2 nN was found. Similarly, the water wettability explored by DCA was found to vary remarkably. Hydrophobic PTFE showed a high advancing contact angle with $\theta_{adv} = 119° \pm 2°$, whereas significantly lower values were observed for TCP ($\theta_{adv} = 22° \pm 1°$) and LAP ($\theta_{adv} = 28° \pm 2°$ (while the non-coated lower site exhibited a contact angle of $\theta_{adv} = 98 \pm 4°$)). These results clearly confirmed that the chosen polymer-based substrates exhibited a similar low surface roughness while its water wettability was different.

Table 1. Surface topography and local mechanical analysis of polymeric substrates.

Material	Reduced Young´s-Modulus E [MPa]	Indentation depth δ [nm]	Pull-off force f_p [nN]	Surface roughness R_q [nm]
PTFE	340 ± 30[a]	345 ± 13[a]	32.3 ± 10[a]	25.0 ± 3.1[a]
TCP	2,500 ± 200[a]	74 ± 1.6[a]	5.2 ± 2[a]	10.2 ± 3.1[a]
LAP	3.5 ± 1.5[b]	214 ± 55[b]	0.6 ± 0.2[b]	8.7 ± 0.7[a]

(Arithmetic mean ± SD)

[a] AFM experiments conducted with cantilever OMCL-AC200TS-R3.

[b] AFM experiments conducted with cantilever MLCT-A. Every determination of E, δ, f_p was performed for n = 10, R_q for n = 3.

3.2. Fate of HUVEC

On PTFE 42 HUVEC were in the vision field (886 µm x 667 µm) at baseline; 10 showed mitotic activity, 14 went into apoptosis and 5 HUVEC left the vision field during the observation period of 72 hours. After the culture medium change, only six of these cells were still adherent in the vision field.

On TCP 82 HUVEC were in the vision field (886 µm x 667 µm) at baseline; 13 HUVEC showed mitotic activity, 6 went into apoptosis and 11 HUVEC left the vision field during the observation period of 72 hours. After the culture medium change, all of these cells were still adherent and could be tracked further.

On LAP 33 HUVEC were in the vision field (886 µm x 667 µm) at baseline; none of these HUVEC showed mitotic activity, none went into apoptosis and 2 HUVEC left the vision field during the observation period of 72 hours. None of the HUVEC in the vision field was still adherent after culture medium change.

The numbers of apoptotic cells as well as the numbers of cells leaving the vision field differed markedly between the three substrates (3*2 contingency table, p = 0.0006, p = 0.0034 respectively).

Only on TCP, did a HUVEC monolayer develop that approached confluence on the third day after seeding (see also Fig. 2B) while on both other materials cells regularly detached (see Fig. 2A, 2C). Figure 2 shows the density of HUVEC on the three polymeric substrates at the end of the observation period of three days. Only on TCP, an optical confluence of nearly 90% was reached. On PTFE only some HUVEC were visible while on LAP no HUVEC were found.

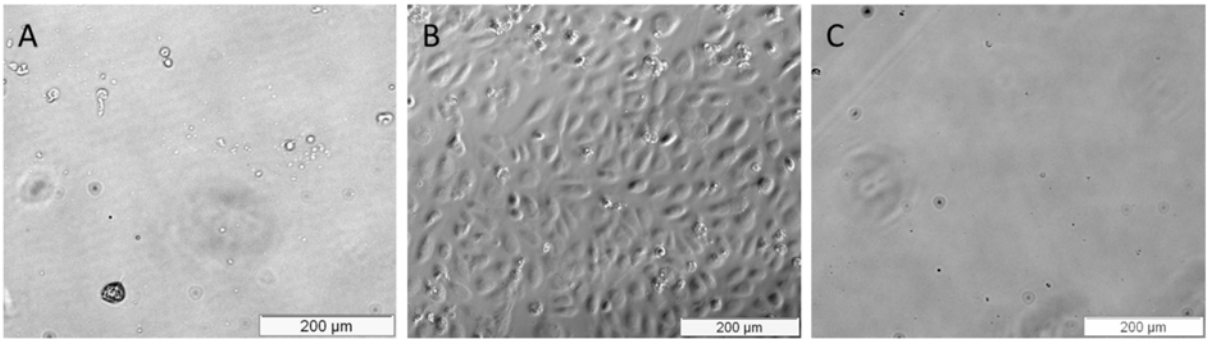

Fig. 2. Microscopic view on endothelial cells adherent on different polymers. Density of adherent endothelial cells on the three materials at the end of the observation period of three days of culture. (A): PTFE, (B): TCP, (C): LAP.

3.3. Length of trajectories

Figure 3 shows the mean length of the trajectories of HUVEC on the three substrates.

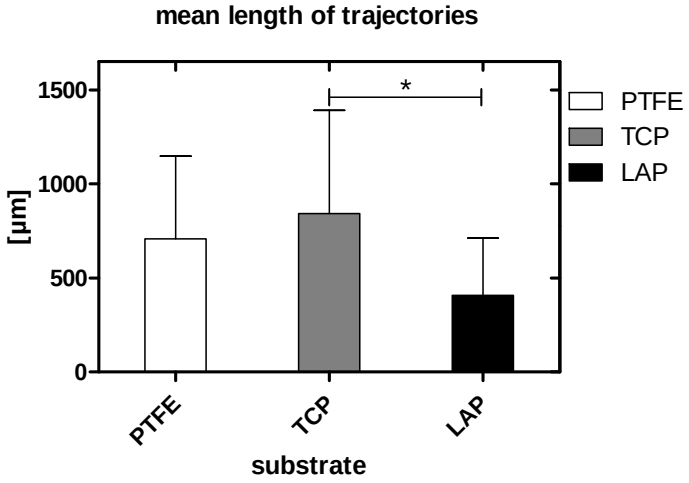

Fig. 3. Mean length of the total trajectories of endothelial cell migration. Total length of the endothelial cell trajectories between starting and end point on PTFE, TCP and LAP over the observation period of three days (arithmetic mean ± standard deviation) (*: $p < 0.05$).

The trajectories differed in their lengths significantly (one factorial ANOVA: $p < 0.001$). Pairwise multiple comparisons showed that the trajectory on PTFE (averaged over 42 HUVEC) was with 710 µm ± 440 µm about 74% longer than on LAP (averaged over 33 HUVEC) with 410 µm ± 300 µm ($p < 0.05$) and the trajectory on TCP (averaged over 82 HUVEC) was with 840 µm ± 550 µm about 106.9% longer than on LAP ($p < 0.05$), while there was no difference in the trajectory lengths between PTFE and TCP ($p > 0.05$).

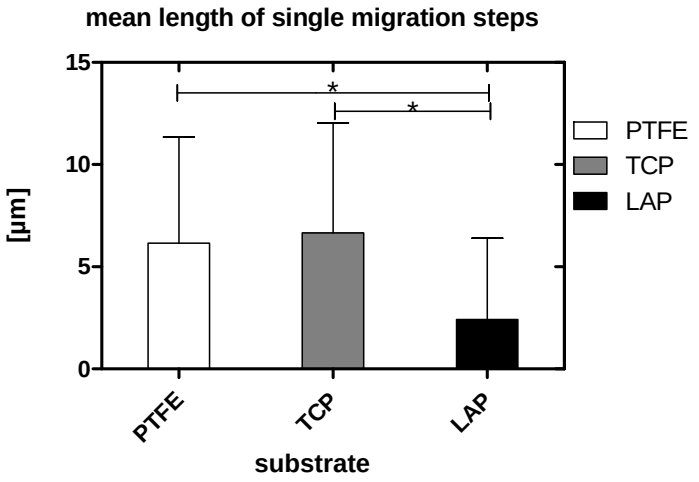

Fig. 4. Mean length of single migration steps on different polymeric substrates. Mean lengths of single migration steps of endothelial cells on PTFE, TCP, and LAP (arithmetic mean ± standard deviation) (*: $p < 0.05$).

3.4. Length of single migration steps

Figure 4 shows the mean length of the single migration steps on the three substrates. The differences of the mean length of the migration steps among the materials were greater than would be expected by chance; there was a statistically significant difference (one factorial ANOVA: $p < 0.001$).

Pairwise multiple comparisons showed that the step length on PTFE (averaged over 5,090 single steps) was with 6.1 µm ± 5.2 µm about more than double as long (231.8% related to the LAP step length) as on LAP (averaged over 5,613 single steps) with 2.4 µm ± 3.9 µm ($p < 0.05$). Also on TCP (averaged over 8,828 single steps) the mean step length was with 6.7 µm ± 5.8 µm nearly threefold longer (274.8% related to the LAP step length) than on LAP ($p < 0.05$). Also, the trajectory on TCP was significantly longer than on PTFE (118.5%, $p > 0.05$).

3.5. Cell velocity during migration

The mean velocities of the HUVEC on the three materials differed markedly and were greater than would be expected by chance (one factorial ANOVA: $p < 0.001$). On PTFE the averaged velocity was 0.40 ± 0.3 µm·min^{-1}, on TCP 0.44 ± 0.3 µm·min^{-1} and on LAP 0.16 ± 0.3 µm·min^{-1}. Pairwise multiple comparisons (Holm-Sidak method) revealed that all three differed from each other ($p = 0.05$ each). After the third day the cells were still moving, though the cell density on TCP was increased after three days nearly reaching optical confluence. On both other substrates only a few cells adhered, on LAP mostly as clusters.

Figure 5 shows the mean migratory velocity of HUVEC and representative examples of the velocities of single HUVEC on PTFE, TCP and LAP over three days. On LAP none of the cells remained adherent over the complete observation time.

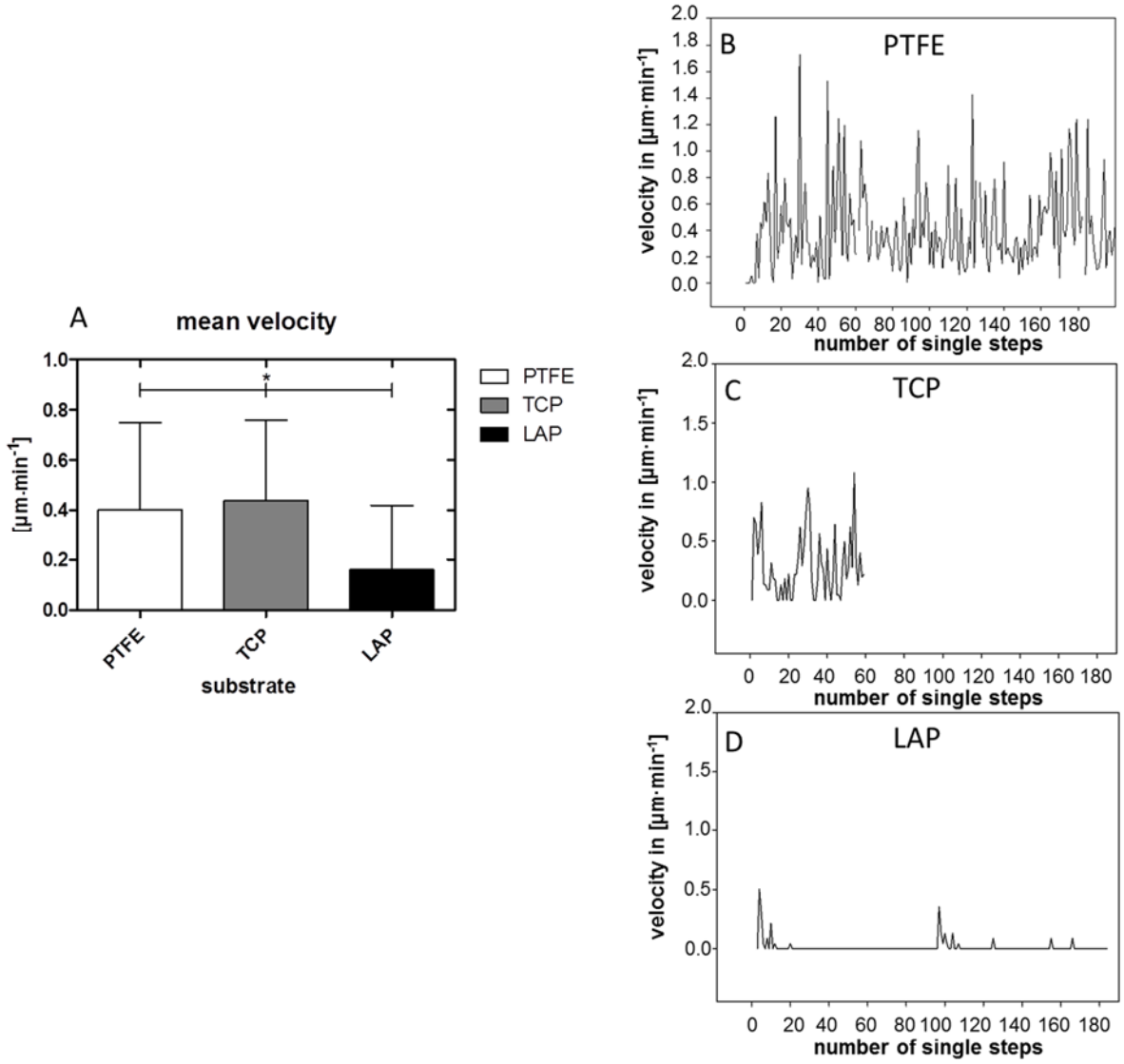

Fig. 5 A: Mean velocities [µm·min^{-1}] of single HUVEC on different polymeric substrates over three days; (B) on PTFE, (C) on TCP and (D) on LAP (*:$p < 0.05$)

3.6. Migration plots

The HUVEC seemed to migrate randomly without any preferred direction on the substrates investigated but showed a markedly different migration pattern (see Fig.1). While the HUVEC on TCP moved with more or less equally long steps, especially on LAP series of very short steps were sometimes followed by steps of very long distance up to some hundred microns

(with some of them leaving the vision field, which then were excluded from the analysis see Fig.1), which obviously occurred after the HUVEC detached from the surface. A similar pattern was observed for HUVEC on PTFE.

3.7. Shape of adherent HUVEC

Figure 6 shows HUVEC on PTFE, TCP, and LAP prior to culture medium change (second day). HUVEC on TCP showed the typical features of attached and migrating HUVEC, they migrated as single cells and presented a polarized (elongated) structure with one front lamella and the retraction of a tail. On both other materials the performance of the HUVEC was completely different. Those HUVEC on LAP were visible as small, round cells or cell debris. The overwhelming majority of cells appeared detached and seriously damaged. A clear locomotion of the cells was not visible. On PTFE only a few HUVEC were attached and visible and a small part of the HUVEC showed a low spread elongated shape with more than one front lamella.

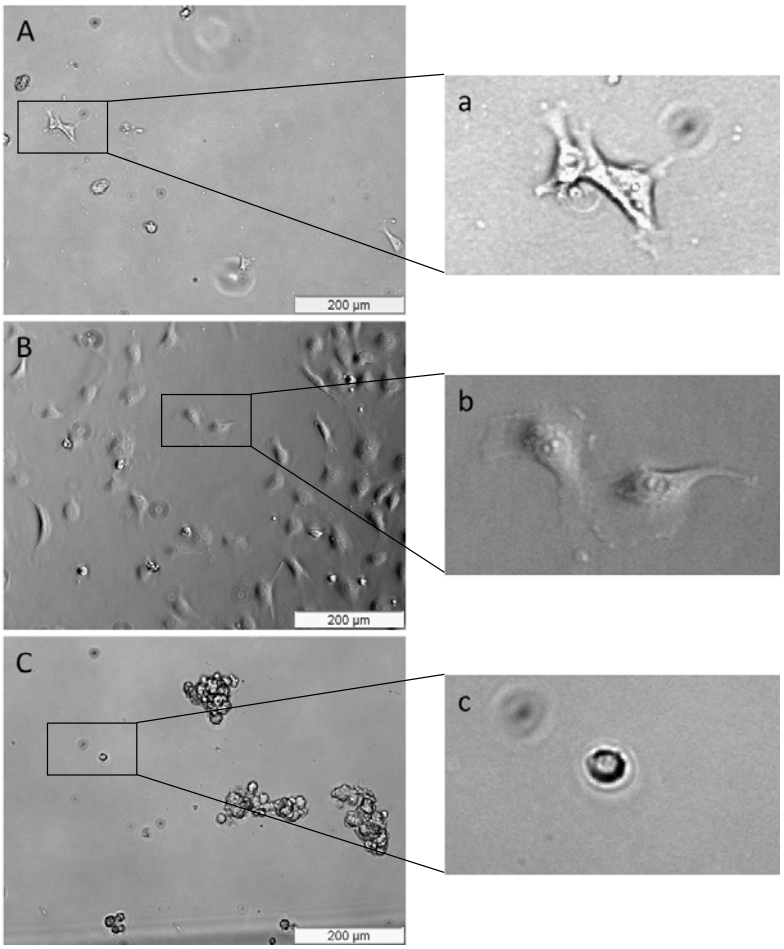

Fig. 6. Representative images of pattern and form of adherent HUVEC on PTFE (A), TCP (B), and LAP (C) prior to culture medium change at the second day (A - C: complete vision field, a- c: magnified details).

3.8. Actin cytoskeleton and focal adhesions

In conjunction with the *in situ* tracking analysis, endpoint immunofluorescence microscopy revealed further insights into the cell processes involved. In HUVEC on TCP as well as on PTFE lots of actin stress fibres in central parts of the cells were visible. The most prominent difference between TCP and PTFE occurred concerning the distribution of vinculin. While on TCP diffuse signals of vinculin were found over the whole basal surface of the cells, on PTFE vinculin was solely arranged at the cell rims (Fig. 7). On the hydrophilic material (LAP (C), $\theta_{adv} = 28° \pm 2°$) no HUVEC were adherent after the culture medium change. Here, only debris of cells and cell nuclei were visible after staining.

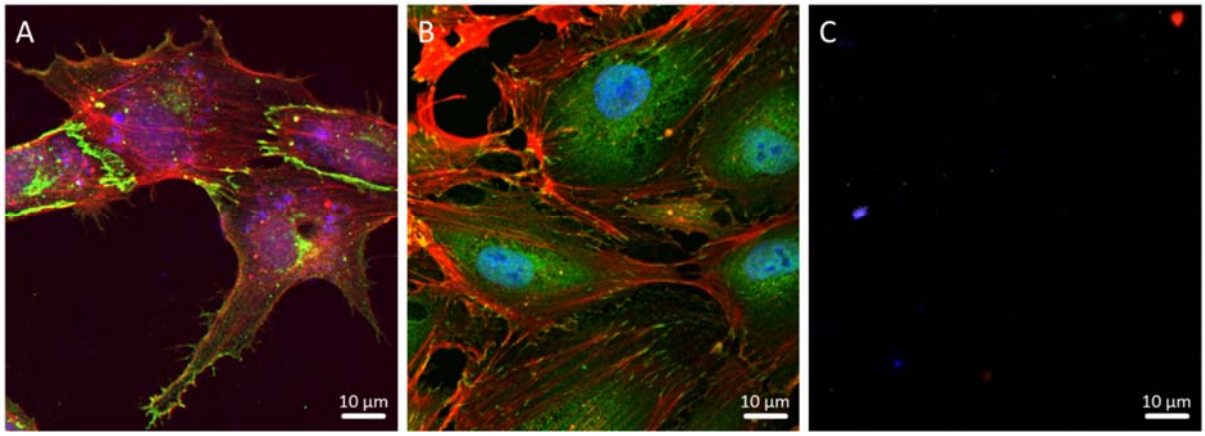

Fig. 7. Representative confocal microscopic images of adherent HUVEC seeded on different materials after three days. HUVEC seeded on PTFE (A), TCP (B) and LAP (C) were fixed with paraformaldehyde. (Red corresponds to F-actin as cytoskeleton marker, green to vinculin as focal adhesion component, blue structures to DAPI labelled nuclei).

3.9. Cell proliferation

The proliferation of $CD31^+$ HUVEC was investigated for non-adherent and adherent cells (Fig. 8). Non-adherent HUVEC showed a low proliferation rate; about 10% of the HUVEC proliferated at day 1 as well at day 3 and there was no difference between the three substrates (two- way ANOVA: $p<0.05$). In contrast, $CD31^+$ HUVEC adherent on TCP showed a significantly increased proliferation rate compared to $CD31^+$ HUVEC on PTFE and LAP (TCP vs LAP d1, TCP vs PTFE d1: $p < 0.01$). Here, more than 50% of the adherent cells were proliferating. HUVEC seeded on LAP showed the lowest number of proliferating cells similar to the proliferation of non-adherent cells.

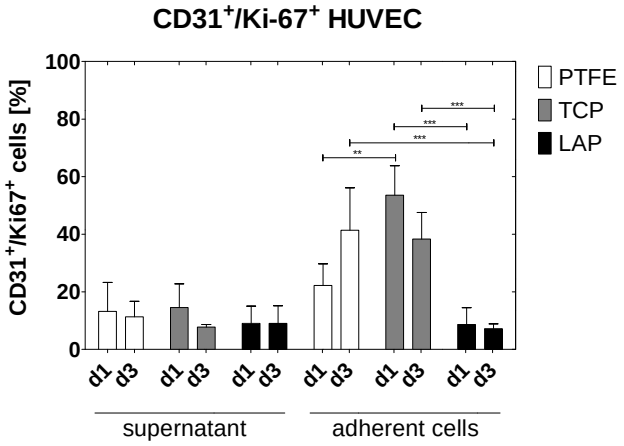

Fig. 8. Percentages of proliferating adherent and non-adherent HUVEC ($CD31^+/Ki\text{-}67^+$ cells) seeded on PTFE, TCP, and LAP (arithmetic mean ± standard deviation). **:$p < 0.01$, ***:$p < 0.001$

3.10. Cytokine release

In the supernatant of HUVEC cultured on the three different substrates a broad range of cytokines known to be synthesized in endothelial cells were measured. Cytokines, which remained below the detection limits, are listed in Table 2 (data not shown).

Table 2. Cytokines with concentrations in the supernatant below the detection limit.

cytokines below detection range			
IL-1ra	IL-1β	IL-2	IL-4
IL-7	IL-9	IL-10	IL-12
IL-15	basic FGF	G-CSF	GM-CSF
RANTES	VEGF	MIP- 1α	MIP- 1β
Eotaxin	TNF-α	IL-17	IFN-γ
IL-5	IL-13		

In the supernatants of HUVEC seeded on TCP and PTFE (Fig. 9) the concentration of monocyte chemoattractant protein-1 (MCP-1) increased markedly after three days of cultivation (two way ANOVA for repeated measures: PTFE vs LAP $p < 0.001$, TCP vs LAP $p < 0.001$, respectively) while in the supernatants of LAP no changes occurred ($p > 0.05$). The highest concentrations were measured in the supernatants of cells cultured on TCP after one as well as after three days of cultivation. Overall, the lowest concentrations were detected for LAP (TCP vs PTFE: d1 $p < 0.01$, d3 $p < 0.001$, TCP vs LAP: d1 $p < 0.001$, d3 $p < 0.001$, LAP vs PTFE d3 $p < 0.001$).

The interleukin 8 concentrations (IL-8) were markedly higher in the supernatants of HUVEC seeded on PTFE and TCP compared to LAP after three days of cultivation (two-way ANOVA for repeated measures: $p < 0.001$ each). The highest concentrations of IL-8 were found in the supernatants of HUVEC seeded on TCP - similar to the results found for MCP-1 (TCP vs PTFE; TCP vs LAP d1, d3 $p < 0.001$).

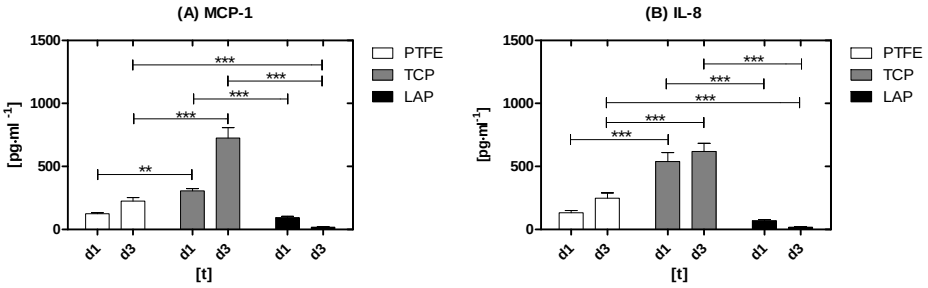

Fig. 9. Chemokines ((A) MCP-1, (B) IL-8) in biologically relevant amounts measured in the supernatants of HUVEC after three days of cultivation on PTFE, TCP, and LAP (arithmetic mean ± standard deviation). **:$p < 0.01$, ***:$p < 0.001$

Table 3 comprises values of cytokines measured in biologically not relevant concentrations.

Table 3. PDGF-BB and IL-6 release by HUVEC measured in the supernatants of HUVEC after three days of cultivation on PTFE, TCP, and LAP (arithmetic mean ± standard deviation; +: $p < 0.05$ compared to PTFE, -: $p < 0.05$ compared to TCP.)

cytokine	Observed concentration in [pg·mL^{-1}]					
	PTFE d1	PTFE d3	TCP d1	TCP d3	LAP d1	LAP d3
PDGF-BB	56.4 ± 22.8	31.7 ± 14.7	26.8 ± 5.6	114.3 ± 53.8^{+}	150.1 ± 66.9^{+-}	37.8 ± 37.8^{-}
IL-6	13.4 ± 3.5	15.0 ± 7.0	30.2 ± 8.9^{+}	34.6± 18.1^{+}	8.4 ± 4.0^{-}	1.3± 0.6^{+-}

4. Discussion

One of the most important tasks of endothelial cells (EC) is to equip the vascular system with an internal non-thrombogenic surface that is regularly renewed to maintain this task and avoiding endothelial dysfunction [45,46]. In addition, EC continuously distribute the blood flow to supply the tissue with oxygen and nutrients by the secretion or the release of vasoactive mediators. To regulate the repair and regeneration of the vascular wall – especially after pathological events like atherosclerotic lesions, trauma or the implantation of cardiovascular devices – EC are endowed with the capacity to migrate towards the injury or the body foreign surface and, after nidation, to proliferate and to seal the injury.

The migration process of HUVEC is influenced by a number of chemical and physical stimuli, including the characteristics of the substratum. In previous studies, surface characteristics of implant materials often were modified using bioactive molecules or polypeptide sequences to optimize the endothelialization [29,47-51]. The binding of proteins covering the body foreign surface e.g. with fibronectin resulted in migration velocities (in the initial stage of 8 µm/h), which under static conditions did not longer depend on the substrate itself [52].

Therefore, in the present study the influence of polymeric substrates with extremely different surface wettabilities – known as important factor of cell-surface interaction [53] - on the migration of HUVEC was exploited [54,55]. The roughness of the three polymers, which were in the low nanometer range, was comparable. The *E*-moduli ranged between 3.5 ± 1.5 MPa for LAP; 340 ± 30 MPa for PTFE and 2,500 ± 200 MPa for TCP. PTFE and TCP as stiff materials should not differently influence the HUVEC-substrate interaction because HUVEC sense elastic tissues *in vivo* [56] in the range of 0.1 to 1 kPa (extracellular matrix [57,58]) or of 100 kPa up to a maximum of 1 MPa in older patients (arterial wall [59]). The hydrogel coating causes LAP to have an elastic modulus comparable to soft tissues. The high water content of the hydrogel obviously hindered the adhesion of EC. However, the nanoindentation measurements revealed that the hydrogel coating was inhomogeneous. Some areas showed E-moduli of 1,500 ± 800 MPa deviating greatly with very high variability, possibly because of significant changes in the thickness of the hydrogel coating. However, a hydrogel coating must have been still present, because EC were also not able to adhere also in these areas.

The adherence and migration pattern of HUVEC differed markedly with respect to the wettability of the polymers. EC generally interact better with hydrophilic (wettable) surfaces than with hydrophobic (non-wettable) ones [27,34,60]. However, the results of the study clearly showed that on the hydrophilic substrate LAP, (θ_{adv} = 28° ± 2°) the HUVEC had difficulties adhering. After seeding 30,000 HUVEC/well on LAP, only 33 cells were visible appearing as non-spread-out, rounded, and very loosely attached cells (Fig. 6) which were no longer present after the culture medium change (Fig. 5) – indicating a very loose binding to the substrate. This could be confirmed by actin/vinculin staining (Fig. 7). After the washing procedure during staining, no HUVEC were found on the LAP surface; only debris of cells and nuclei were visible after 72 h. The corona treatment process of TCP generates highly energetic oxygen ions, which graft onto the surface polystyrene chains so that the surface becomes hydrophilic. The more oxygen that is incorporated on to the surface the more hydrophilic it becomes and the better it is for cell attachment and spreading [61]. It is important to note, that LAP was coated with a hydrogel, and thus presents as a water film consisting of chemically bound water molecules. In

contrary, the water film on TCP should have been very thin consisting of only some physically bound molecule layers. Many reports have emphasized the role of hydration and water structure in protein and cell adsorption [62]. It seems to be very likely that both effects – called the water barrier hypothesis [7] – might explain our results. The water molecules in the swollen hydrogel - consisting of only some percent of polymer – do not provide required densities of binding sites for the EC. In contrary, EC can easily displace physically bound water molecules on TCP so that the cells can adhere to the polymer surface. The migration analysis revealed that the cells moved on the LAP surface only over very small distances then detached, adhered loosely again with a next short migration period. At a higher magnification it could clearly be seen that the performance of those cells was completely different from that what is described as migration: The cells stayed in their round non-spread-out shape and protruded very small and short filipodia – an active locomotion with the formation of a front lamella and the retraction of a tail was not visible [63,64] - then they moved over very short distances mostly around 1 µm (but also steps up to 5 micron were found). The mean step length was with 2.4 ± 3.9 µm significantly shorter than on both other polymers, which was also the case for the complete trajectory length. The low number of proliferating cells also suggests that no physiological migration took place. It is well-known that anchorage-dependent cells like HUVEC are not able to proliferate unless they attach and spread on a substratum [53]. Also the release of chemokines was minimal and did not reach levels which were biologically active.

On the hydrophobic polymer (PTFE, contact angle 119°) - which is in clinical use as vascular graft material - 42 out of 30,000 HUVEC attached initially in the area of the vision field of 886 µm x 667 µm of the hydrophobic material and could be tracked. Some of these cells showed a spread-out elongated shape, which usually is visible for migrating cells but formed more than one lamella and that in different directions. The other HUVEC attached on PTFE appeared as small, well rounded, spherical cells indicating a low binding to the hydrophobic substrate and no migratory activity was seen. This was mirrored by the shorter mean trajectory length compared to HUVEC on TCP. After staining actin and vinculin, it became clear, why the HUVEC on PTFE only loosely adhered. Vinculin is a membrane-cytoskeletal protein in focal adhesions that is involved in linkage of integrin adhesion molecules to the actin cytoskeleton [65]. Vinculin is associated with cell-cell and cell-matrix junctions anchoring F-actin to the membrane. Figure 7 clearly shows that vinculin in cells on PTFE is concentrated at the rim of the HUVEC leading to a cell-cell binding but only very few binding sites to the cell-substrate are visible at the basal membrane of the HUVEC. A loss of vinculin disrupts the anchorage of actin filaments to the membrane, and reduces cell adhesion and spreading so that the binding

of the HUVEC to the substrate is low [66]. The adhering HUVEC could migrate and also proliferate (see Fig. 8) but they detached regularly, what explains the low HUVEC density at the end of the observation period (Fig. 5) though a high percentage of the adherent HUVEC – at day 3 more than 40% – presented the Ki-67 protein which is strictly associated with cell proliferation [67].

Surface treated polystyrene substrate (TCP), which is widely used in cell biology and biotechnology, was proved to be very wetting with an advancing contact angle of $\theta_{adv} = 22° \pm 1°$. On this substrate 82 out of 30,000 HUVEC attached initially to the surface of the hydrophobic material and 71 of them remained attached in the vision field and could be tracked over the three days of observation. All of these cells presented the typical spread polarized structure, which usually is visible for migrating cells with one front lamella and the retraction of a tail [63,64]. The vinculin staining (see Fig. 7B) revealed lots of diffusively spread signals of vinculin over the whole basal surface of the cells, which was completely different from the distribution of vinculin in HUVEC on PTFE or even more on LAP. In addition, stress fibres in central parts of HUVEC oriented in parallel to the cell axis ended in vinculin stained focal adhesions demonstrating the good anchorage of the HUVEC to the TCP substrate. All of the cells migrated and over 50% were proliferating explaining the nearly 90% optical confluence at the end of the third day after seeding.

Chemokines are chemotactic cytokines - which are critical for inflammation-induced trafficking of blood cells during wound healing and might be involved in the adhesion, migration, proliferation or inflammatory process during endothelialization - were measured, too. A key chemokine that regulates migration is the monocyte chemoattractant protein-1 (MCP-1) involved in the inflammatory response after vascular wall injury [68,69]. MCP-1 attracts monocytes *in vitro* at subnanomolar concentrations [70,71]. Figure 9 demonstrates that MCP-1 is released in biologically active concentrations from HUVEC cultured on TCP, which is in line with former studies showing that MCP-1 is increased during repair or regeneration of injured tissue [68,69,72]. On both other polymers the concentrations of MCP-1 were far below values described to be significant *in vivo* [73].

Very similar results were found according to the release of IL-8 another chemokine, associated with inflammation. IL-8 causes neutrophil migration to the site of injury and intensifies the migration and proliferation of endothelial cells and in an autocrine manner further amplifying the migration [74]. In addition, this chemokine was markedly higher in supernatants of HUVEC on TCP compared to the supernatants of HUVEC seeded on PTFE or LAP. Because of the auto- and paracrine effects of both chemokines on HUVEC, it is likely that they have contributed to

the migration behaviour and, ultimately, the rapid formation of HUVEC monolayers on TCP of nearly 90% after three days.

All other cyto - and chemokines measured were either below the detection range or did not reach concentrations to be biologically active. In addition, one should have in mind, that on PTFE and especially on LAP markedly less cells adhered (and proliferated) than on TCP, what might also contribute to the very low concentrations measured in the supernatants of these cell cultures.

Since there were no chemotactic gradients on the surfaces the HUVEC migrated randomly without any preferred directions as expected and shown in former studies [75].

5. Conclusion

The polymers with different water wettabilities resulted in diverse migration, adhesion and proliferation of HUVECs. The averaged length of the trajectories as well as the mean step length of single migrating HUVEC differed markedly between the three polymers. Only on TCP the migration, adherence and proliferation performance of HUVEC resulted in nearly confluent HUVEC monolayers. Neither the hydrophilic (LAP) nor the hydrophobic (PTFE) substrate allowed the development of HUVEC monolayers because there was an impaired migration, almost no adherence and no proliferation on LAP and only rare adherence on PTFE although proliferation markers were slightly enhanced.

This demonstrates that in initial states of interaction the wettability of the substrate governed the migratory process as well as the adhesion of EC, which is of importance for the proliferation and endothelialization of polymer-based biomaterials. These results were supported by immunofluorescence microscopy, which clearly demonstrated that only on TCP a sufficient binding of the HUVEC on the substrate developed. In addition, the chemokine analysis revealed that the HUVEC released MCP-1 and IL-8 only on TCP, which can further amplify the migration and proliferation.

Acknowledgements

The authors thank the Helmholtz Association for funding through Impuls- und Vernetzungsfond SO-036, through grant no. VH-VI-423 (Helmholtz Virtual Institute “Multifunctional Biomaterials for Medicine”), through programme-oriented funding, as well as through a fellowship for Wan Yan by the Helmholtz Graduate School for Macromolecular

Bioscience (VH-GS-503). Anne Krüger-Genge was recipient of a fellowship of the Helmholtz Postdoc Program 2012 (PD-064).

References

[1] Task Force Members, Montalescot G, Sechtem U, Achenbach S, Andreotti F, Arden C, Budaj A, Bugiardini R, Crea F, Cuisset T, Di Mario C, Ferreira JR, Gersh BJ, Gitt AK, Hulot JS, Marx N, Opie LH, Pfisterer M, Prescott E, Ruschitzka F, Sabate M, Senior R, Taggart DP, van der Wall EE, Vrints CJ, E. S. C. Committee for Practice Guidelines, Zamorano JL, Achenbach S, Baumgartner H, Bax JJ, Bueno H, Dean V, Deaton C, Erol C, Fagard R, Ferrari R, Hasdai D, Hoes AW, Kirchhof P, Knuuti J, Kolh P, Lancellotti P, Linhart A, Nihoyannopoulos P, Piepoli MF, Ponikowski P, Sirnes PA, Tamargo JL, Tendera M, Torbicki A, Wijns W, Windecker S, Document R, Knuuti J, Valgimigli M, Bueno H, Claeys MJ, Donner-Banzhoff N, Erol C, Frank H, Funck-Brentano C, Gaemperli O, Gonzalez-Juanatey JR, Hamilos M, Hasdai D, Husted S, James SK, Kervinen K, Kolh P, Kristensen SD, Lancellotti P, Maggioni AP, Piepoli MF, Pries AR, Romeo F, Ryden L, Simoons ML, Sirnes PA, Steg PG, Timmis A, Wijns W, Windecker S, Yildirir A, Zamorano JL. 2013 ESC guidelines on the management of stable coronary artery disease: The Task Force on the management of stable coronary artery disease of the European Society of Cardiology, Eur. Heart J. 2013; 34(38): 2949-3003.

[2] Fontana A, Spadaro S, Copetti M, Spoto B, Salvemini L, Pizzini P, Frittitta L, Mallamaci F, Pellegrini F, Trischitta V, Menzaghi C. Association between Resistin Levels and All-Cause and Cardiovascular Mortality: A New Study and a Systematic Review and Meta-Analysis, PLoS One 2015; 10(3): e0120419.

[3] Perek B, Malinska A, Stefaniak S, Ostalska-Nowicka D, Misterski M, Zabel M, Suri A, Nowicki M. Predictive Factors of Late Venous Aortocoronary Graft Failure: Ultrastructural Studies, PLoS One 2013; 8(8): e70628.

[4] Menu P, Stoltz JF, Kerdjoudj H. Progress in vascular graft substitute, Clin. Hemorheol. Microcirc. 2013; 53(1-2): 117-29.

[5] Remy M, Bareille R, Rerat V, Bourget C, Marchand-Brynaert J, Bordenave L. Polyethylene terephthalate membrane grafted with peptidomimetics: Endothelial cell compatibility and retention under shear stress, J. Biomater. Sci., Polym. Ed. 2013; 24(3): 269-86.

[6] Clowes AW, Gown AM, Hanson SR, Reidy MA. Mechanisms of arterial graft failure. 1. Role of cellular proliferation in early healing of PTFE prostheses, Am. J. Pathol. 1985; 118(1): 43-54.

[7] Lee BS, Shin HS, Park K, Han DK. Surface grafting of blood compatible zwitterionic poly(ethylene glycol) on diamond-like carbon-coated stent, J. Mater. Sci.: Mater. Med. 2011; 22(3): 507-14.

[8] Neffe AT, von Ruesten-Lange M, Braune S, Luetzow K, Roch T, Richau K, Jung F, Lendlein A. Poly(ethylene glycol) Grafting to Poly(ether imide) Membranes: Influence on Protein Adsorption and Thrombocyte Adhesion, Macromol. Biosci. 2013; 13(12): 1720-1729.

[9] Wei Y, Ji Y, Xiao L-L, Lin Q-K, Xu J-P, Ren K-F, Ji J. Surface engineering of cardiovascular stent with endothelial cell selectivity for in vivo re-endothelialisation, Biomaterials 2013; 34(11): 2588-2599.

[10] Mayer A, Roch T, Kratz K, Lendlein A, Jung F. Pro-angiogenic CD14++ CD16+ CD163+ monocytes accelerate the in vitro endothelialization of soft hydrophobic poly(n-butyl acrylate) networks, Acta Biomater. 2012; 8(12): 4253-4259.

[11] Tseng C-N, Karlof E, Chang Y-T, Lengquist M, Rotzius P, Berggren P-O, Hedin U, Eriksson EE. Contribution of Endothelial Injury and Inflammation in Early Phase to Vein Graft Failure: The Causal Factors Impact on the Development of Intimal Hyperplasia in Murine Models, PLoS One 2014; 9(6): e98904.
[12] Schulz C, Hecht J, Krüger-Genge A, Kratz K, Jung F, Lendlein A. Generating Aptamers Interacting with Polymeric Surfaces for Biofunctionalization, Macromol. Biosci. 2016; 16(12): 1776-1791.
[13] Örtenwall P, Wadenvik H, Kutti J, Risberg B. Endothelial cell seeding reduces thrombogenicity of Dacron grafts in humans, J. Vasc. Surg. 1990; 11(3): 403-10.
[14] Bordenave L, Menu P, Baquey C. Developments towards tissue-engineered, small-diameter arterial substitutes, Expert Rev. Med. Devices 2008; 5(3): 337-47.
[15] Deutsch M, Meinhart J, Zilla P, Howanietz N, Gorlitzer M, Froeschl A, Stuempflen A, Bezuidenhout D, Grabenwoeger M. Long-term experience in autologous in vitro endothelialization of infrainguinal ePTFE grafts, Journal of Vascular Surgery 2009; 49(2): 352-362.
[16] Vara DS, Salacinski HJ, Kannan RY, Bordenave L, Hamilton G, Seifalian AM. Cardiovascular tissue engineering: State of the art, Pathol. Biol. 2005; 53(10): 599-612.
[17] Jay PY, Pham PA, Wong SA, Elson EL. A mechanical function of myosin II in cell motility, J. Cell Sci. 1995; 108 (Pt 1)(387-93.
[18] Bellion A, Baudoin JP, Alvarez C, Bornens M, Metin C. Nucleokinesis in tangentially migrating neurons comprises two alternating phases: Forward migration of the Golgi/centrosome associated with centrosome splitting and myosin contraction at the rear, J. Neurosci. 2005; 25(24): 5691-9.
[19] Janson LW, Taylor DL. In vitro models of tail contraction and cytoplasmic streaming in amoeboid cells, J. Cell Biol. 1993; 123(2): 345-56.
[20] Paluch E, Sykes C, Prost J, Bornens M. Dynamic modes of the cortical actomyosin gel during cell locomotion and division, Trends Cell Biol. 2006; 16(1): 5-10.
[21] Gimbrone MA Jr. Culture of vascular endothelium, Prog. Hemostasis Thromb. 1976; 3: 1-28.
[22] Zygourakis K, Bizios R, Markenscoff P. Proliferation of anchorage-dependent contact-inhibited cells: I. Development of theoretical models based on cellular automata, Biotechnol. Bioeng. 1991; 38(5): 459-70.
[23] Sato Y, Rifkin DB. Autocrine activities of basic fibroblast growth factor: Regulation of endothelial cell movement, plasminogen activator synthesis, and DNA synthesis, J. Cell Biol. 1988; 107(3): 1199-205.
[24] Balja F, Blatter M-C, James RW, Pometta D, Gabbiani G. Actin stress fiber content of regenerated endothelial cells correlates with intramural retention of intermediate plus low density lipoproteins in rat aorta after balloon injury, Atherosclerosis 1989; 76(2–3): 181-191.
[25] Dieterich P, Odenthal-Schnittler M, Mrowietz C, Krämer M, Sasse L, Oberleithner H, Schnittler HJ. Quantitative morphodynamics of endothelial cells within confluent cultures in response to fluid shear stress, Biophys. J. 2000; 79(3): 1285-1297.
[26] Franke RP, Gräfe M, Schnittler H, Seiffge D, Mittermayer C, Drenckhahn D. Induction of human vascular endothelial stress fibres by fluid shear stress, Nature 1984; 307(5952): 648-649.
[27] Hiebl B, Cui J, Kratz K, Frank O, Schossig M, Richau K, Lee S, Jung F, Lendlein A. Viability, Morphology and Function of Primary Endothelial Cells on Poly(n-Butyl Acrylate) Networks Having Elastic Moduli Comparable to Arteries, J. Biomater. Sci., Polym. Ed. 2012; 23(7): 901-915.

[28] Klein-Soyer C, Azorsa DO, Cazenave JP, Lanza F. CD9 participates in endothelial cell migration during in vitro wound repair, Arterioscler., Thromb., Vasc. Biol. 2000; 20(2): 360-9.
[29] Schnittler HJ, Franke RP, Akbay U, Mrowietz C, Drenckhahn D. Improved in vitro rheological system for studying the effect of fluid shear stress on cultured cells, Am. J. Physiol. 1993; 265(1): C289-C298.
[30] Sohn H-Y, Krotz F, Gloe T, Keller M, Theisen K, Klauss V, Pohl U. Differential regulation of xanthine and NAD(P)H oxidase by hypoxia in human umbilical vein endothelial cells. Role of nitric oxide and adenosine, Cardiovasc. Res. 2003; 58(3): 638-646.
[31] Pan L, Liu C, Kong Y, Piao Z, Cheng B. Phentolamine inhibits angiogenesis in vitro: Suppression of proliferation, migration and differentiation of human endothelial cells, Clinical Hemorheology and Microcirculation 2017; 65: 31-41.
[32] Cheng Q, Lee BL, Komvopoulos K, Yan Z, Li S. Plasma surface chemical treatment of electrospun poly(L-lactide) microfibrous scaffolds for enhanced cell adhesion, growth, and infiltration, Tissue Eng., Part A 2013; 19(9-10): 1188-98.
[33] Griesser HJ, Chatelier RC, Gengenbach TR, Johnson G, Steele JG. Growth of human cells on plasma polymers: Putative role of amine and amide groups, J. Biomater. Sci., Polym. Ed. 1994; 5(6): 531-554.
[34] Grinnell F, Milam M, Srere PA. Studies on cell adhesion. II. Adhesion of cells to surfaces of diverse chemical composition and inhibition of adhesion by sulfhydryl binding reagents, Arch. Biochem. Biophys. 1972; 153(1): 193-8.
[35] Horbett TA, Schway MB, Ratner BD. Hydrophilic-hydrophobic copolymers as cell substrates: Effect on 3T3 cell growth rates, J. Colloid Interface Sci. 1985; 104(1): 28-39.
[36] Schakenraad JM, Busscher HJ, Wildevuur CRH, Arends J. The influence of substratum surface free energy on growth and spreading of human fibroblasts in the presence and absence of serum proteins, J. Biomed. Mater. Res. 1986; 20(6): 773-784.
[37] Shen M, Horbett TA. The effects of surface chemistry and adsorbed proteins on monocyte/macrophage adhesion to chemically modified polystyrene surfaces, J Biomed Mater Res 2001; 57(3): 336-45.
[38] Ridley AJ, Schwartz MA, Burridge K, Firtel RA, Ginsberg MH, Borisy G, Parsons JT, Horwitz AR. Cell migration: Integrating signals from front to back, Science 2003; 302(5651): 1704-9.
[39] Anonymus. Ethical guidelines for publication in Clinical Hemorheology and Microcirculation: Update 2016, Clinical Hemorheology and Microcirculation 2016; 63: 1-2.
[40] Hiebl B, Lützow K, Lange M, Jung F, Seifert B, Klein F, Weigel T, Kratz K, Lendlein A. Cytocompatibility testing of cell culture modules fabricated from specific candidate biomaterials using injection molding, J. Biotechnol. 2010; 148(1): 76-82.
[41] Yoshikawa HY, Cui J, Kratz K, Matsuzaki T, Nakabayashi S, Marx A, Engel U, Lendlein A, Tanaka M. Quantitative evaluation of adhesion of osteosarcoma cells to hydrophobic polymer substrate with tunable elasticity, J. Phys. Chem. B 2012; 116(28): 8024-30.
[42] Lauffenburger DA, Horwitz AF. Cell migration: A physically integrated molecular process, Cell 1996; 84(3): 359-69.
[43] Stokes CL, Lauffenburger DA, Williams SK. Migration of individual microvessel endothelial cells: Stochastic model and parameter measurement, J. Cell Sci. 1991; 99 (Pt 2): 419-30.

[44] Abràmoff MD, Magalhães PJ, Ram SJ. Image processing with ImageJ, Biophotonics International 2004; 11(7): 36-43.
[45] Feletou M, Editor. The Endothelium: Part 1: Multiple Functions of the Endothelial Cells-Focus on Endothelium-Derived Vasoactive Mediators, San Rafael (CA), 2011.
[46] Gori T, von Henning U, Muxel S, Schaefer S, Fasola F, Vosseler M, Schnorbus B, Binder H, Parker JD, Münzel T. Both flow-mediated dilation and constriction are associated with changes in blood flow and shear stress: Two complementary perspectives on endothelial function, Clinical Hemorheology and Microcirculation 2016; 64: 255-266.
[47] Ceylan H, Tekinay AB, Guler MO. Selective adhesion and growth of vascular endothelial cells on bioactive peptide nanofiber functionalized stainless steel surface, Biomaterials 2011; 32(34): 8797-8805.
[48] Hoshi RA, Van Lith R, Jen MC, Allen JB, Lapidos KA, Ameer G. The blood and vascular cell compatibility of heparin-modified ePTFE vascular grafts, Biomaterials 2013; 34(1): 30-41.
[49] Plant SD, Grant DM, Leach L. Behaviour of human endothelial cells on surface modified NiTi alloy, Biomaterials 2005; 26(26): 5359-5367.
[50] Pratt BM, Harris AS, Morrow JS, Madri JA. Mechanisms of cytoskeletal regulation. Modulation of aortic endothelial cell spectrin by the extracellular matrix, Am. J. Pathol. 1984; 117(3): 349-354.
[51] Yang Z, Tu Q, Maitz MF, Zhou S, Wang J, Huang N. Direct thrombin inhibitor-bivalirudin functionalized plasma polymerized allylamine coating for improved biocompatibility of vascular devices, Biomaterials 2012; 33(32): 7959-7971.
[52] Pompe T, Kobe F, Salchert K, Jorgensen B, Oswald J, Werner C. Fibronectin anchorage to polymer substrates controls the initial phase of endothelial cell adhesion, J. Biomed. Mater. Res., Part A 2003; 67(2): 647-57.
[53] Stoker M, O'Neill C, Berryman S, Waxman V. Anchorage and growth regulation in normal and virus-transformed cells, Int. J. Cancer 1968; 3(5): 683-93.
[54] Gilbert PM, Havenstrite KL, Magnusson KE, Sacco A, Leonardi NA, Kraft P, Nguyen NK, Thrun S, Lutolf MP, Blau HM. Substrate elasticity regulates skeletal muscle stem cell self-renewal in culture, Science 2010; 329(5995): 1078-81.
[55] Rae PJ, Dattelbaum DM. The properties of poly(tetrafluoroethylene) (PTFE) in compression, Polymer 2004; 45(22): 7615-7625.
[56] Discher D, Dong C, Fredberg JJ, Guilak F, Ingber D, Janmey P, Kamm RD, Schmid-Schonbein GW, Weinbaum S. Biomechanics: Cell research and applications for the next decade, Ann. Biomed. Eng. 2009; 37(5): 847-59.
[57] Engler AJ, Sweeney HL, Discher DE, Schwarzbauer JE. Extracellular matrix elasticity directs stem cell differentiation, J. Musculoskeletal Neuronal Interact. 2007; 7(4): 335.
[58] Reilly GC, Engler AJ. Intrinsic extracellular matrix properties regulate stem cell differentiation, J. Biomechanics 2010; 43(1): 55-62.
[59] Satija M, Yadav TP, Sachdev N, Chhabra A, Jahan A, Dewan V. Endothelial function, arterial wall mechanics and intima media thickness in juvenile idiopathic arthritis, Clin. Exp. Rheumatol. 2014; 32(3): 432-9.
[60] Spijker HT, Graaff R, Boonstra PW, Busscher HJ, van Oeveren W. On the influence of flow conditions and wettability on blood material interactions, Biomaterials 2003; 24(26): 4717-27.
[61] Ramsey WS, Hertl W, Nowlan ED, Binkowski NJ. Surface treatments and cell attachment, In Vitro 1984; 20(10): 802-8.
[62] Liu XL, Yuan L, Li D, Tang ZC, Wang YW, Chen GJ, Chen H, Brash JL. Blood compatible materials: State of the art, J Mater Chem B 2014; 2(35): 5718-5738.

[63] Giannone G, Dubin-Thaler BJ, Rossier O, Cai Y, Chaga O, Jiang G, Beaver W, Dobereiner HG, Freund Y, Borisy G, Sheetz MP. Lamellipodial actin mechanically links myosin activity with adhesion-site formation, Cell 2007; 128(3): 561-75.
[64] Kajstura J, Bereiter-Hahn J. Loss of focal contacts accompanies the density dependent inhibition of cell growth, Cell Biol. Int. Rep. 1989; 13(4): 377-83.
[65] Geiger B. A 130K protein from chicken gizzard: Its localization at the termini of microfilament bundles in cultured chicken cells, Cell 18(1): 193-205.
[66] Xu W, Baribault H, Adamson ED. Vinculin knockout results in heart and brain defects during embryonic development, Development 1998; 125(2): 327-37.
[67] Scholzen T, Gerdes J. The Ki-67 protein: From the known and the unknown, J. Cell. Physiol. 2000; 182(3): 311-22.
[68] Dewald O, Zymek P, Winkelmann K, Koerting A, Ren G, Abou-Khamis T, Michael LH, Rollins BJ, Entman ML, Frangogiannis NG. CCL2/Monocyte Chemoattractant Protein-1 Regulates Inflammatory Responses Critical to Healing Myocardial Infarcts, Circ. Res. 2005; 96(8): 881-889.
[69] Otsuka F, Finn AV, Yazdani SK, Nakano M, Kolodgie FD, Virmani R. The importance of the endothelium in atherothrombosis and coronary stenting, Nat. Rev. Cardiol. 2012; 9(8): 439-453.
[70] Leonard EJ, Yoshimura T. Human monocyte chemoattractant protein-1 (MCP-1), Immunol. Today 1990; 11(3): 97-101.
[71] Rollins BJ. Monocyte chemoattractant protein 1: A potential regulator of monocyte recruitment in inflammatory disease, Molecular medicine today 1996; 2(5): 198-204.
[72] Wood S, Jayaraman V, Huelsmann EJ, Bonish B, Burgad D, Sivaramakrishnan G, Qin S, Dipietro LA, Zloza A, Zhang C, Shafikhani SH. Pro-inflammatory chemokine CCL2 (MCP-1) promotes healing in diabetic wounds by restoring the macrophage response, PLoS One 2014; 9(3): e91574.
[73] Ding D, Su D, Li X, Li Z, Wang Y, Qiu J, Lin P, Zhang Y, Guo P, Xia M, Li D, Yang Y, Hu G, Ling W. Serum Levels of Monocyte Chemoattractant Protein-1 and All-Cause and Cardiovascular Mortality among Patients with Coronary Artery Disease, PLoS One 2015; 10(3): e0120633.
[74] Waugh DJJ, Wilson C. The Interleukin-8 Pathway in Cancer, Clin. Cancer Res. 2008; 14(21): 6735-6741.
[75] Lee Y, McIntire LV, Zygourakis K. Analysis of endothelial cell locomotion: Differential effects of motility and contact inhibition, Biotechnology and Bioengineering 1994; 43(7): 622-634.